REPORT DOCUMENTATION PAGE

Form Approved OMB NO. 0704-0188

1. REPORT DATE (DD-MM-YYYY)	2. REPORT TYPE	3. DATES COVERED (From - To)
03-11-2022	Final Report	1-Oct-2017 - 31-Jul-2022

4. TITLE AND SUBTITLE
Final Report: A Cross-Disciplinary Investigation of Amorphous-Crystalline Ceramics Synthesized Using Far-From-Equilibrium Electromagnetic Excitations

5a. CONTRACT NUMBER
W911NF-17-1-0589

5b. GRANT NUMBER

5c. PROGRAM ELEMENT NUMBER
611102

6. AUTHORS

5d. PROJECT NUMBER

5e. TASK NUMBER

5f. WORK UNIT NUMBER

7. PERFORMING ORGANIZATION NAMES AND ADDRESSES
Carnegie Mellon University
Associate Director, Sponsored Programs
5000 Forbes Avenue
Pittsburgh, PA 15213 -3890

8. PERFORMING ORGANIZATION REPORT NUMBER

9. SPONSORING/MONITORING AGENCY NAME(S) AND ADDRESS (ES)
U.S. Army Research Office
P.O. Box 12211
Research Triangle Park, NC 27709-2211

10. SPONSOR/MONITOR'S ACRONYM(S)
ARO

11. SPONSOR/MONITOR'S REPORT NUMBER(S)
71215-SM-YIP.6

12. DISTRIBUTION AVAILIBILITY STATEMENT
Approved for public release; distribution is unlimited.

13. SUPPLEMENTARY NOTES
The views, opinions and/or findings contained in this report are those of the author(s) and should not contrued as an official Department of the Army position, policy or decision, unless so designated by other documentation.

14. ABSTRACT

15. SUBJECT TERMS

16. SECURITY CLASSIFICATION OF:			17. LIMITATION OF ABSTRACT	15. NUMBER OF PAGES	19a. NAME OF RESPONSIBLE PERSON
a. REPORT	b. ABSTRACT	c. THIS PAGE			B. Reeja Jayan
UU	UU	UU	UU		19b. TELEPHONE NUMBER 412-268-4343

RPPR Final Report
as of 07-Nov-2022

Agency Code: 21XD

Proposal Number: 71215SMYIP **Agreement Number: W911NF-17-1-0589**
INVESTIGATOR(S):

Name: B. Reeja Jayan
Email: bjayan@andrew.cmu.edu
Phone Number: 4122684343
Principal: Y

Organization: **Carnegie Mellon University**
Address: Associate Director, Sponsored Programs, Pittsburgh, PA 152133890
Country: USA

DUNS Number: 052184116 EIN: 250969449
Report Date: 31-Oct-2022 Date Received: 03-Nov-2022
Final Report for Period Beginning 01-Oct-2017 and Ending 31-Jul-2022
Title: A Cross-Disciplinary Investigation of Amorphous-Crystalline Ceramics Synthesized Using Far-From-Equilibrium Electromagnetic Excitations
Begin Performance Period: 01-Oct-2017 **End Performance Period:** 31-Jul-2022
Report Term: 0-Other

Submitted By: B. Reeja Jayan Email: bjayan@andrew.cmu.edu
Phone: (412) 268-4343

Distribution Statement: 1-Approved for public release; distribution is unlimited.

STEM Degrees: 3 **STEM Participants:** 4

Major Goals: The goal of this project is to find direct evidence for non-thermal interactions between matter and EM waves, and to model such interactions to enrich our scientific understanding. We seek to investigate and engineer these low temperature, far-from-equilibrium effects of electromagnetic fields to synthesize materials unavailable to conventional routes.

To achieve this goal, the project is divided into the following 3 scientific objectives:

1. To experimentally measure the localized temperatures induced by selective EM field interaction with precursor materials during synthesis.

2. To conduct in situ, in operando investigations to determine how EM fields alter the Gibbs free energy of activation and/or the pre-exponential factor during the nucleation, crystallization, and growth processes.

3. To synergistically use experiments and computational models to identify far-from-equilibrium effects of EM fields and their relationships with field parameters (e.g., field intensity, polarization, frequency).

See attached report file for further details.

Accomplishments: Please see attached PDF file for details

RPPR Final Report
as of 07-Nov-2022

Training Opportunities: Postdoctoral Fellow: Shikhar Jha (2018-2019)
Project Title: Defect-mediated Anisotropic Lattice Expansion of Ceramics as Evidence for Non-thermal Coupling between Electromagnetic Fields and Matter
Department of Mechanical Engineering, Carnegie Mellon University.
*Now an Assistant Professor at Indian Institute of Technology (IIT), Kanpur, India

PhD Thesis: Shuyan Zhang (Defending on Dec 5, 2022)
Co-adviser – Prof. Alan McGaughey
Project Title: Analyzing total X-ray scattering data with atomistic simulation and machine learning
Department of Mechanical Engineering, Carnegie Mellon University (CMU).
*Will tentatively start as Postdoctoral Fellow at Jayan Lab, CMU in Spring 2023.

PhD student: Malik Blackman (2019-2021)
Co-adviser – Prof. Jonathan Malen
Project Title: Laser Thermoreflectance measurement of local temperatures under microwave exposure
Department of Mechanical Engineering, Carnegie Mellon University (CMU).
*Did not pass PhD qualifying exam

Undergraduate student: Colby Sisco (2021-2022)
Project Title: Flow-through Reactor Engineering for microwave Pump-X-ray probe time-resolved studies
Department of Mechanical Engineering, Carnegie Mellon University (CMU).
*Currently working in Jayan Lab

RPPR Final Report
as of 07-Nov-2022

Results Dissemination: List of Peer Reviewed Publications & Selected Presentations from YIP project Student, post-doc on project are underlined.

1. S. K. Jha, N. Nakamura, S. Zhang, L. Su, P. M. Smith, X. L. Phuah, H. Wang, J. S. Okasinski, A. J. H. McGaughey, B. Reeja?Jayan, “Defect-mediated Anisotropic Lattice Expansion of Ceramics as Evidence for Non-thermal Coupling between Electromagnetic Fields and Matter,” Advanced Engineering Materials 21, 1900762 (2019)

2. B. Reeja-Jayan and J. Luo “Far-from-equilibrium effects of electric and electromagnetic fields in ceramics synthesis and processing,” MRS Bulletin, 46, 26 (2021). Guest Editor for the January 2021 Issue on Synthesis and Processing Under Electric/Electromagnetic Fields.

3. S. Zhang, J. Gong, S. Chu, D. Xiao, B. Reeja-Jayan, and A. J. McGaughey, “Pair distribution function analysis driven by atomistic simulations: Application to microwave radiation synthesized TiO2 and ZrO2,” arXiv preprint arXiv:2210.05890 (2022).

4. S. Zhang, J. Gong, S. Chu, D. Xiao, B. Reeja-Jayan, and A. J. McGaughey, “Pair distribution function analysis for oxide defect identification through feature extraction and supervised learning,” arXiv preprint arXiv:2210.07371 (2022).

5. S. Zhang, J. Gong, B. Reeja-Jayan, A.J. McGaughey, "Data-driven approaches on pair distribution function data: matrix factorization and clustering," Foundations of Crystallography, 77, C190 (2021).

6. S. Zhang, J. Gong, B. Reeja-Jayan, A.J. McGaughey, “Data-driven approaches on pair distribution function (PDF) data”, International Union of Crystallography (IUCr), Aug 14-22, 2021.

7. S. Zhang, J. Gong, S.K. Jha, N. Nakamura, B. Reeja-Jayan, A.J. McGaughey, “Structures of point defects in titanium dioxide in microwave-assisted synthesis”, Materials Research Society (MRS), Nov 28 - Dec 4, 2020.
8. S. Zhang, J. Gong, S.K. Jha, N. Nakamura, B. Reeja-Jayan, A.J. McGaughey, “Structures of point defects in titanium dioxide in microwave-assisted synthesis”, International Mechanical Engineering Congress & Exposition (IMECE), Nov 16 - 19, 2020.

9. S. Zhang, J. Gong, S.K. Jha, N. Nakamura, B. Reeja-Jayan, A.J. McGaughey, “Structures of point defects in titanium dioxide in microwave-assisted synthesis”, Material Science & Technology (MS&T), Nov 2 - 6, 2020.
10. S. Zhang, N. Nakamura, J. Gong, B. Reeja-Jayan, A.J. McGaughey, “Structures of point defects in titanium dioxide in microwave-assisted synthesis”, Electronic Materials Conference (EMC), Jun 24-26, 2020.

11. “Engineering Ceramic Based Materials for Energy and Sustainability”, Invited talk, European Materials Research Society (E-MRS), Virtual Meeting, 30 May- 3 Jun 2022.

12. “Engineering Far-From-Equilibrium Materials Using Electromagnetic Fields,” Invited Speaker, Chemical Engineering, Cornell University, 25 Oct 2021.

13. “Engineering Far-From-Equilibrium Materials Using Electromagnetic Fields,” Keynote Speaker, Annual Convention of the Deutsche Forschungsgemeinschaft (DFG, German Research Foundation), 2 Nov 2021.

14. “Engineering Far-From-Equilibrium Materials Using Electromagnetic Fields”, Invited talk in Rustum Roy Symposium, Materials Science & Technology Conference & Exhibition (MS&T20), Virtual Meeting, USA, 2-6 Nov 2020.

15. “Engineering Far-From-Equilibrium Materials Using Electromagnetic Fields,” Keynote Lecture, Materials Science & Engineering (MSE) Congress of the German Materials Society, Virtual Meeting, 24 Sep 2020.

16. B. Reeja Jayan, “Engineering Far-From-Equilibrium Materials Using Electromagnetic Fields,” Invited Speaker, Basic Research Forum, US Department of Defense, 13 Feb 2020.

RPPR Final Report
as of 07-Nov-2022

Honors and Awards: Awards received by PI B. Reeja Jayan during reporting period of grant (not necessarily related to this project):

Invited to serve on US National Academy of Sciences (NAS) review panel, invited to serve on the Beamtime Advisory Board of the High Energy X-ray (HEX) beamline at Brookhaven National Laboratory, Secretary-elect for the Electronics Division of the American Ceramic Society (2022), CMU Engineering Dean's Early Career Fellow (one of two winners in 2020), 54th Annual Keynote Speaker, International Microwave Power Institute (IMPI, 2020), Invited attendee at 2020 Roundtable on Biomedical Engineering Materials and Applications (BEMA), US National Academy of Engineering (NAE), U.S. Department of Energy (DOE) Faculty Research Program Participant - National Energy Technology Laboratory (NETL), ORISE/ORAU 2020, Faculty Fellow, Scott Institute for Energy Innovation (2019), George Tallman Ladd Research Award (2019), National Science Foundation (NSF) CAREER Award (2018).

*Promoted to Associate Professor of Mechanical Engineering at Carnegie Mellon University; effective 1 July, 2020

Protocol Activity Status:

Technology Transfer: Nothing to Report

PARTICIPANTS:

Participant Type: Postdoctoral (scholar, fellow or other postdoctoral position)
Participant: Shikhar Jha
Person Months Worked: 15.00 **Funding Support:**
Project Contribution:
National Academy Member: N

Participant Type: Graduate Student (research assistant)
Participant: Shuyan Zhang
Person Months Worked: 15.00 **Funding Support:**
Project Contribution:
National Academy Member: N

Participant Type: Graduate Student (research assistant)
Participant: Malik Blackman
Person Months Worked: 6.00 **Funding Support:**
Project Contribution:
National Academy Member: N

Participant Type: Undergraduate Student
Participant: Colby Sisco
Person Months Worked: 6.00 **Funding Support:**
Project Contribution:
National Academy Member: N

Participant Type: PD/PI
Participant: B. Reeja Jayan
Person Months Worked: 6.00 **Funding Support:**
Project Contribution:
National Academy Member: N

RPPR Final Report
as of 07-Nov-2022

ARTICLES:

Publication Type: Journal Article Peer Reviewed: Y **Publication Status:** 1-Published
Journal: Advanced Engineering Materials
Publication Identifier Type: DOI Publication Identifier: 10.1002/adem.201900762
Volume: 21 Issue: 12 First Page #: 1900762
Date Submitted: 8/29/20 12:00AM Date Published: 8/30/19 12:00PM
Publication Location:
Article Title: Defect-mediated Anisotropic Lattice Expansion in Ceramics as Evidence for Non-thermal Coupling Between Electromagnetic Fields and Matter
Authors: Shikhar K. Jha, Nathan Nakamura, Shuyan Zhang, Laisuo Su, Phil M. Smith, Xin L. Phuah, Han Wang,
Keywords: Ceramics, low temperature processing, microwave synthesis, defect generation, in-situ synchrotron X-ray diffraction, non-thermal effects, anisotropic lattice expansion
Abstract: Electromagnetic (EM) fields can trigger a range of surprising responses in materials. Microwave radiation (MWR), a type of EM field in the frequency range of 0.3– 300GHz, can lower the synthesis temperature required for ceramics such as TiO2 and induces mixed amorphous–crystalline phase compositions. To better understand the effects of MWR on matter, structural changes during microwave heating andMWR-assisted synthesis using in situ synchrotron X-ray diffraction are studied. Anisotropic expansion–contraction of lattice parameters under microwave-radiation is observed, which contradicts the results fromconventional thermal heating. When as-received TiO2 powders are heated with MWR, an instantaneous decrease in the intensities of diffraction peaks indicates decrystallization/amorphization. Highresolution electron microscopy supports these observations. Raman spectroscopy and X-ray photoemission spectroscopy indicate increased defect-generation under microwave exposure. Molecular dynamics
Distribution Statement: 2-Distribution Limited to U.S. Government agencies only; report contains proprietary info
Acknowledged Federal Support: **Y**

Publication Type: Journal Article Peer Reviewed: Y **Publication Status:** 1-Published
Journal: MRS Bulletin
Publication Identifier Type: DOI Publication Identifier: 10.1557/s43577-020-00009-9
Volume: 46 Issue: 1 First Page #: 26
Date Submitted: 2/10/21 12:00AM Date Published: 1/1/21 5:00AM
Publication Location:
Article Title: Far-from-equilibrium effects of electric and electromagnetic fields in ceramics synthesis and processing
Authors: B. Reeja-Jayan, Jian Luo
Keywords: Sintering, Microwave heating, Ceramic, Multiscale
Abstract: Electric and electromagnetic fields can promote far-from-equilibrium chemical reactions, phase transformations, and microstructural evolution. On the one hand, both direct electric fields and time-varying electromagnetic fields can change the atomic and microscale structure of materials in ways that differ from conventional methods. On the other hand, ultrafast densification in a matter of seconds (e.g., in flash sintering) and electrically induced microstructural evolution open up new opportunities for materials processing. In many cases, the external fields absorbed within a material may result in “nonthermal” effects. In other cases, thermal effects dominate, but applied fields can still influence the microstructural evolution or generate nonequilibrium defects. Consequently, new behavior evolves such as ceramics that become ductile due to high densities of dislocations created by the far-from-equilibrium processing. Many open scientific questions remain about the fundamental mecha
Distribution Statement: 2-Distribution Limited to U.S. Government agencies only; report contains proprietary info
Acknowledged Federal Support: **Y**

RPPR Final Report
as of 07-Nov-2022

Publication Type: Journal Article Peer Reviewed: N **Publication Status:** 5-Submitted
Journal: Physical Review Materials (submitted)
Publication Identifier Type: Publication Identifier:
Volume: Issue: First Page #:
Date Submitted: 8/31/21 12:00AM Date Published:
Publication Location:
Article Title: Atomistic simulation for structure model generation in pair distribution function analysis: application to microwave radiation synthesized TiO2 and ZrO2
Authors: Shuyan Zhang, Jie Gong, Daniel Xiao, B. Reeja Jayan, and Alan J. H. McGaughey
Keywords: molecular dynamics, defects
Abstract: We have employed atomistic simulations in the structure model generation in pair distribution function (PDF) analysis to study the atomic structures with local disorder.
Distribution Statement: 2-Distribution Limited to U.S. Government agencies only; report contains proprietary info
Acknowledged Federal Support: **Y**

Publication Type: Journal Article Peer Reviewed: N **Publication Status:** 5-Submitted
Journal: APL Machine Learning (submitted)
Publication Identifier Type: Other Publication Identifier:
Volume: Issue: First Page #:
Date Submitted: 11/3/22 12:00AM Date Published:
Publication Location:
Article Title: Pair distribution function analysis for oxide defect identification through feature extraction and supervised learning
Authors: Shuyan Zhang, Jie Gong, Sharon Chu, Daniel Xiao, B. Reeja Jayan, Alan J. H. McGaughey
Keywords: defects, machine learning
Abstract: Feature extraction and a neural network model are applied to predict the defect types and concentrations in experimental TiO2 samples. A dataset of TiO2 structures with vacancies and interstitials of oxygen and titanium is built and the structures are relaxed using energy minimization. The features of the calculated pair distribution functions (PDFs) of these defected structures are extracted using linear methods (principal component analysis, non-negative matrix factorization) and non-linear methods (autoencoder, convolutional neural network). The extracted features are used as the inputs to a neural network that maps the feature weights to the concentration of each defect type. The performance of this machine learning pipeline is validated by predicting the defect concentrations based on experimentally-measured TiO2 PDFs and comparing the results to brute-force predictions. A physics-based initialization of the autoencoder has the highest accuracy in predicting defect concentration.
Distribution Statement: 2-Distribution Limited to U.S. Government agencies only; report contains proprietary info
Acknowledged Federal Support: **Y**

RPPR Final Report
as of 07-Nov-2022

Publication Type: Journal Article Peer Reviewed: N **Publication Status:** 5-Submitted
Journal: Computational Materials Science
Publication Identifier Type: Publication Identifier:
Volume: Issue: First Page #:
Date Submitted: 11/3/22 12:00AM Date Published:
Publication Location:
Article Title: Pair distribution function analysis driven by atomistic simulations: Application to microwave radiation synthesized TiO2 and ZrO2
Authors: Shuyan Zhang, Jie Gong, Daniel Xiao, B. Reeja Jayan, Alan J. H. McGaughey
Keywords: Molecular dynamics, defects
Abstract: A workflow is presented for performing pair distribution function (PDF) analysis of defected materials using structures generated from atomistic simulations. A large collection of structures, which differ in the types and concentrations of defects present, are obtained through energy minimization with an empirical interatomic potential. Each of the structures is refined against an experimental PDF. The structures with the lowest goodness of fit Rw values are taken as being representative of the experimental structure. The workflow is applied to anatase titanium dioxide (a-TiO2) and tetragonal zirconium dioxide (t-ZrO2) synthesized in the presence of microwave radiation, a low temperature process that generates disorder. The results suggest that titanium vacancies and interstitials are the dominant defects in a-TiO2, while oxygen vacancies dominate in t-ZrO2. Analysis of the atomic displacement parameters extracted from the PDF refinement and mean squared displacements calculated from m
Distribution Statement: 2-Distribution Limited to U.S. Government agencies only; report contains proprietary info
Acknowledged Federal Support: **Y**

Partners

,

I certify that the information in the report is complete and accurate:
Signature: B. Reeja Jayan
Signature Date: 11/3/22 3:16PM

Final Report – October 2022

A Cross-Disciplinary Investigation of Amorphous-Crystalline Ceramics Synthesized Using Far-From-Equilibrium Electromagnetic Excitations

Principle Investigator: B. Reeja Jayan, Associate Professor, Carnegie Mellon University

1. Abstract and Project Goal

The goal of this project is to find direct evidence for non-thermal interactions between matter and EM waves, and to model such interactions to enrich our scientific understanding. *We seek to investigate and engineer these low temperature, far-from-equilibrium effects of electromagnetic fields to synthesize materials unavailable to conventional routes.*

To achieve this goal, the project is divided into the following 3 scientific objectives:

1. To experimentally measure the localized temperatures induced by selective EM field interaction with precursor materials during synthesis.
2. To conduct *in situ, in operando* investigations to determine how EM fields alter the Gibbs free energy of activation and/or the pre-exponential factor during the nucleation, crystallization, and growth processes.
3. To synergistically use experiments and computational models to identify far-from-equilibrium effects of EM fields and their relationships with field parameters (e.g., field intensity, polarization, frequency).

Unlike radiative heating from conventional furnace, microwave radiation interacts with the bulk of material and causes volumetric heating. This is not a simple case of transient heating where the knowledge of boundary conditions and material properties can determine the temperature distribution. The temperature variation in bulk would change the response of material, which will cause further inhomogeneity in temperature. In the absence of the knowledge of this localized temperature distribution, the contribution of thermal versus non-thermal effect of microwave becomes difficult to determine. **The novelty of our experimental approach lies in utilizing a thin film of conducting materials (sensitizers such as indium tin oxide ITO or metals like Au) on a glass substrate that creates a preferential site for nucleation**. As glass does not couple well with microwave (2.45 GHz, our experimental frequency), the conducting film becomes an active surface for nucleation for powder synthesis.

During our experiments, we coat a glass slide with ITO/Au and submerged it into the growth solution of tetrabutyl orthotitanate sol-gel combined with tetraethylene glycol (TEG), mixed in the volumetric ratio of 1:4. When the solution is heated up with the microwave, ceramic oxides such as anatase (TiO_2) starts to nucleate on the ITO/Au film preferentially. The solution reached a temperature of 160 °C, as measured by Infrared temperature sensor, which was found to be nearly 300 °C lower than the temperature needed for crystallizing anatase (TiO_2) in conventional settings. While the temperature estimation of solution by infrared (IR) sensor is accurate to be ± 5 °C, the local temperature at ITO/Au surface (nucleation site) remains uncertain. In this project, we seek to determine the effect of localized interaction of the microwave with sensitizer and local heating. We combine experiments, multiscale computational models, and data based machine learning

approaches to study how interface structures (e.g., sensitizer layer on glass) and defects can influence driven structural transformations in materials exposed to microwave radiation.

2. Summary of Accomplishments

- Our coupled *in-situ* experiments using synchrotron X-ray diffraction based temperature measurements and atomistic molecular dynamics (MD) simulations provided direct experimental evidence for non-thermal coupling between externally applied microwave fields and the unit cell of a crystal. **Fig. 7 is the one of the key contributions of this project and shows the anisotropic expansion-contraction of the a and c lattice parameters followed by *de-crystallization (loss of long-range atomic order)* in the anatase TiO2 unit cell under 2.45 GHz microwave heating [Paper 1].** A conventionally heated TiO2 unit cell shows linear relationship between the values of a, c and the temperature of the sample. Our MD model (Fig. 8) suggests that defects (on both Ti and O sub-lattices) are responsible for these anisotropic effects.

- We performed **seminal experiments using laser thermoreflectance** to measure local rise in temperature of a gold thin film on a silicon wafer while exposed to 2.45 GHz radiation inside a microwave reactor. The surface temperature was spike by up to 250^{o}C on the gold sensitizer layer. Such local temperature rises have only been hypothesized (and modeled using COMSOL), but never previously measured.

- We developed a coupled experiment-computation-machine learning workflow to rapidly analyze high throughput synchrotron x-ray total scattering data during in-situ nanomaterial synthesis experiments to identify the type of defect(s) in the structure. Our cross-disciplinary approach **[Papers 3,4]** forms the basis of an **autonomous materials synthesis platform** being proposed for commissioning at the NSLS-II 28-ID-2 beamline at DOE's Brookhaven National Laboratory. These efforts will continue to create impact beyond the timeline of this project.

- PI Jayan guest led an **MRS Bulletin** **[Paper 2]** article about the work done on this project, which introduced the broader materials community to the non-equilibrium effects happening under electric and electromagnetic fields. She also guest edited the January 2021 themed issue of the Bulletin.

The following personnel were trained:

Postdoctoral Fellow: Shikhar Jha (2018-2019)
Project Title: Defect-mediated Anisotropic Lattice Expansion of Ceramics as Evidence for Non-thermal Coupling between Electromagnetic Fields and Matter
Department of Mechanical Engineering, Carnegie Mellon University.
*Now an Assistant Professor at Indian Institute of Technology (IIT), Kanpur, India

PhD Thesis: Shuyan Zhang (*Defending on Dec 5, 2022***)**
Co-adviser – Prof. Alan McGaughey
Project Title: Analyzing total X-ray scattering data with atomistic simulation and machine learning

Department of Mechanical Engineering, Carnegie Mellon University (CMU).
*Will tentatively start as Postdoctoral Fellow at Jayan Lab, CMU in Spring 2023.

PhD student: Malik Blackman (2019-2021)
Co-adviser – Prof. Jonathan Malen
Project Title: Laser Thermoreflectance measurement of local temperatures under microwave exposure
Department of Mechanical Engineering, Carnegie Mellon University (CMU).
*Did not pass PhD qualifying exam

Undergraduate student: Colby Sisco (2021-2022)
Project Title: Flow-through Reactor Engineering for microwave Pump-X-ray probe time-resolved studies
Department of Mechanical Engineering, Carnegie Mellon University (CMU).
*Currently working in Jayan Lab

Awards received by PI B. Reeja Jayan during reporting period of grant (not necessarily related to this project): Invited to serve on US National Academy of Sciences (NAS) review panel, invited to serve on the Beamtime Advisory Board of the High Energy X-ray (HEX) beamline at Brookhaven National Laboratory, Secretary-elect for the Electronics Division of the American Ceramic Society (2022), CMU Engineering Dean's Early Career Fellow (one of two winners in 2020)**,** 54th Annual Keynote Speaker, International Microwave Power Institute (IMPI, 2020)**,** Invited attendee at 2020 Roundtable on Biomedical Engineering Materials and Applications (BEMA), US National Academy of Engineering (NAE), U.S. Department of Energy (DOE) Faculty Research Program Participant - National Energy Technology Laboratory (NETL), ORISE/ORAU, Faculty Fellow, Scott Institute for Energy Innovation (2019), George Tallman Ladd Research Award (2019)**,** National Science Foundation (NSF) CAREER Award (2018).
*Promoted to Associate Professor of Mechanical Engineering at Carnegie Mellon University; effective 1 July, 2020

List of Peer Reviewed Publications & Selected Presentations from YIP project

Student, post-doc on project are underlined.

1. **S. K. Jha**, N. Nakamura, **S. Zhang**, L. Su, P. M. Smith, X. L. Phuah, H. Wang, J. S. Okasinski, A. J. H. McGaughey, B. Reeja-Jayan, "Defect-mediated Anisotropic Lattice Expansion of Ceramics as Evidence for Non-thermal Coupling between Electromagnetic Fields and Matter," *Advanced Engineering Materials* 21, 1900762 (2019)

2. B. Reeja-Jayan and J. Luo "Far-from-equilibrium effects of electric and electromagnetic fields in ceramics synthesis and processing," *MRS Bulletin*, 46, 26 (2021). ***Guest Editor for the January 2021 Issue on Synthesis and Processing Under Electric/Electromagnetic Fields.***

3. **S. Zhang**, J. Gong, S. Chu, D. Xiao, B. Reeja-Jayan, and A. J. McGaughey, "Pair distribution function analysis driven by atomistic simulations: Application to microwave radiation synthesized TiO2 and ZrO2," *arXiv preprint arXiv:2210.05890* (2022).

4. **S. Zhang**, J. Gong, S. Chu, D. Xiao, B. Reeja-Jayan, and A. J. McGaughey, "Pair distribution function analysis for oxide defect identification through feature extraction and supervised learning," *arXiv preprint arXiv:2210.07371* (2022).

5. **S. Zhang**, J. Gong, B. Reeja-Jayan, A.J. McGaughey, "Data-driven approaches on pair distribution function data: matrix factorization and clustering," *Foundations of Crystallography*, 77, C190 (2021).
6. **S. Zhang,** J. Gong, B. Reeja-Jayan, A.J. McGaughey, "Data-driven approaches on pair distribution function (PDF) data", International Union of Crystallography (IUCr), Aug 14-22, 2021.
7. **S. Zhang,** J. Gong, **S.K. Jha**, N. Nakamura, B. Reeja-Jayan, A.J. McGaughey, "Structures of point defects in titanium dioxide in microwave-assisted synthesis", Materials Research Society (MRS), Nov 28 - Dec 4, 2020.
8. **S. Zhang,** J. Gong, **S.K. Jha**, N. Nakamura, B. Reeja-Jayan, A.J. McGaughey, "Structures of point defects in titanium dioxide in microwave-assisted synthesis", International Mechanical Engineering Congress & Exposition (IMECE), Nov 16 - 19, 2020.
9. **S. Zhang,** J. Gong, **S.K. Jha**, N. Nakamura, B. Reeja-Jayan, A.J. McGaughey, "Structures of point defects in titanium dioxide in microwave-assisted synthesis", Material Science & Technology (MS&T), Nov 2 - 6, 2020.
10. **S. Zhang,** N. Nakamura, J. Gong, B. Reeja-Jayan, A.J. McGaughey, "Structures of point defects in titanium dioxide in microwave-assisted synthesis", Electronic Materials Conference (EMC), Jun 24-26, 2020.
11. "Engineering Ceramic Based Materials for Energy and Sustainability", *Invited talk,* **European Materials Research Society (E-MRS)**, Virtual Meeting, 30 May- 3 Jun 2022.
12. "Engineering Far-From-Equilibrium Materials Using Electromagnetic Fields," *Invited Speaker*, Chemical Engineering, **Cornell University**, 25 Oct 2021.
13. "Engineering Far-From-Equilibrium Materials Using Electromagnetic Fields," *Keynote Speaker*, Annual Convention of the **Deutsche Forschungsgemeinschaft (DFG, German Research Foundation)**, 2 Nov 2021.
14. "Engineering Far-From-Equilibrium Materials Using Electromagnetic Fields", *Invited talk in Rustum Roy Symposium,* **Materials Science & Technology Conference & Exhibition (MS&T20)**, Virtual Meeting, USA, 2-6 Nov 2020.
15. "Engineering Far-From-Equilibrium Materials Using Electromagnetic Fields," *Keynote Lecture,* **Materials Science & Engineering (MSE) Congress of the German Materials Society**, Virtual Meeting, 24 Sep 2020.
16. B. Reeja Jayan, "Engineering Far-From-Equilibrium Materials Using Electromagnetic Fields," *Invited Speaker*, Basic Research Forum, **US Department of Defense**, 13 Feb 2020.

3. Technical accomplishments

In this section of this final report, we describe technical accomplishments on Objectives 1 - 3.

*Please note that due to COVID-19 related shut down at the x-ray synchrotron beamline, our synchrotron experimental work on Objectives 2 and 3 was suspended from early 2020 until mid-2021. Accordingly, some tasks related to the in-situ experiments in Objectives 2-3 are being wrapped up in December 2022 and the final two manuscripts will be written in 2022-23. Since the project has ended, PI Jayan is using her discretionary funding from CMU to support this pending work.

<u>Objective 1</u> proposed to experimentally measure the local temperature induced by microwave radiation. Our first task involved setting up Laser Thermoreflectance measurement set-up and performing calibrations.

Since the microwave reacts with metals, conventional thermocouples cannot be used to measure the surface temperature. A non-contacting and non-destructive optical approach of laser thermoreflectance was used to measure the transient surface temperature to ensure that the measurement will not be affected by the microwave. This method has advantage over IR thermometry since the laser can pass through the glass wall and be focused to a spot size of 10 μm on the gold surface.

Thermoreflectance measurement is based on the change in surface reflectivity as a function of temperature. We have chosen a gold film for its high electronic conductivity to act as a sensitizer, and it has the strongest thermoreflectance modulations at the wavelength of the laser used for these measurements, Fig 1a.

We focus a 532 nm wavelength continuous wave probe laser onto a sensitizer (gold) while it is being selectively heated up with the microwave. As the temperature of gold surface increases, its reflectance (R) drops according to the equation 1,

$$R(T) = R_o(1 + \beta(\lambda)\Delta T) \qquad (1)$$

where $\beta(\lambda)$ is the coefficient of thermoreflectance of gold sensitized at a wavelength λ and ΔT is the change in sensitizer surface temperature.

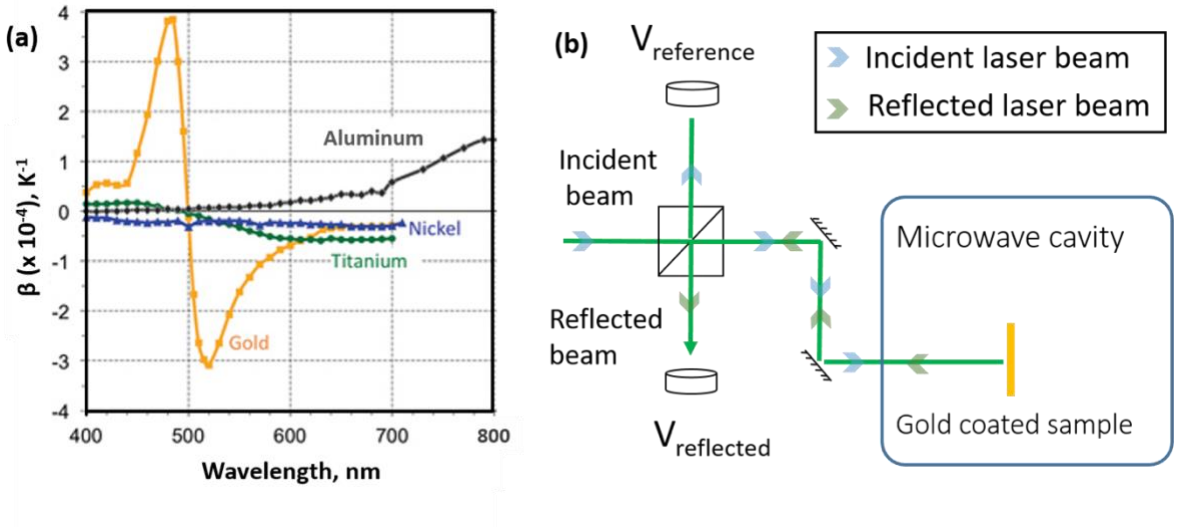

Figure 1. (a) Thermoreflectance coefficient as a function of wavelength for different metals. Gold has the highest modulus, which makes it more susceptive to small changes in temperature. (b) The current experimental set up for laser thermoreflectance measurement.

The schematic set up of our laser thermometry has been shown in Fig. 1(b). The laser probe is directed into a non-polarized 50-50 beam splitter, which directs the half of the beam to the reference photodiode and the other half to the specimen surface. The reflected beam from gold surface passes through the beam splitter to another photodiode. The difference in the normalized

beam intensities (change in reflectance) is proportional to the change in surface temperature of the gold layer, as can be derived from equation 1.

$$\frac{R(T)-R_o}{R_o} = \beta(\lambda).\Delta T = \frac{V_{reflected}-V_{reference}}{V_{reference}} \quad (2)$$

Here, $V_{reflected}$ and $V_{reference}$ measure the intensity of reflected and incident laser beam intensities respectively. We started with the calibration curve where a gold coated silicon wafer was glued to a stage heater, and heated up to 100°C at a step of 10°C for every acquisition. The heating-cooling cycle was repeated to obtain a consistent calibration, as shown in Fig. 2(a). Another calibration, called temperature jump test, involved cycling between two temperatures (40°C and 80°C), as shown in Fig. 2(b). The thermoreflectance coefficient in these two cases were found to be in close agreement with each other.

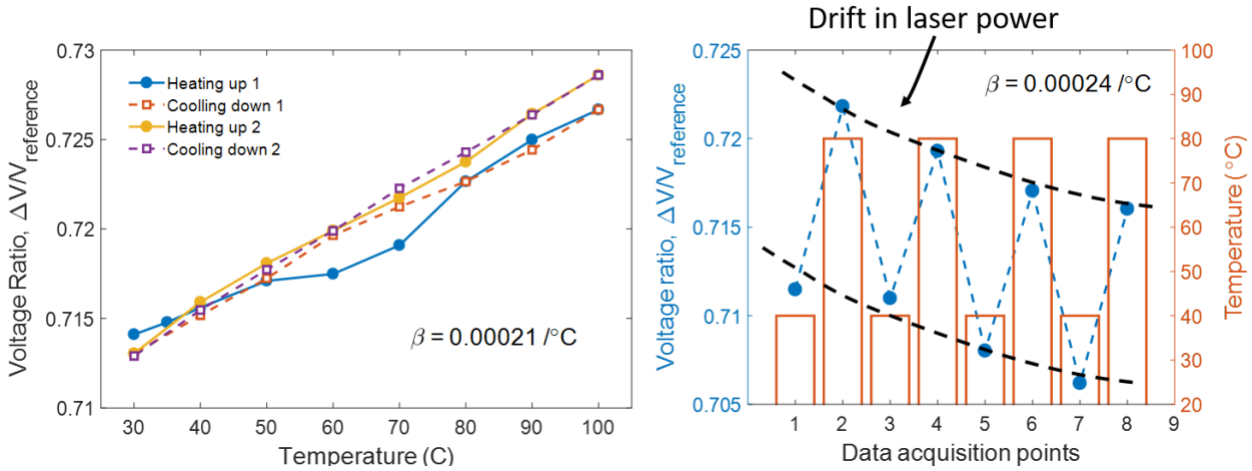

Figure 2. Temperature calibration curve to determine the thermoreflectance coefficient from (a) temperature ramp experiments and (b) temperature jump experiments.

Once we stabilized the calibration, we determined the thermoreflectance coefficient. After this we started making measurements of temperature under the microwave field exposure in our newly designed microwave reactor using a custom-designed set up. We placed a gold-coated glass slide in the middle of a domestic microwave cavity and switched on the microwave for 1 minute. Various ON/OFF cycles were made as seen in Fig. 3 (left). An immediate rise in voltage ratio was measured in response to the microwave heating, as shown in Fig 3 (right). The rise in surface temperature was estimated to be 250°C, which then cooled off exponentially by natural convection with a time constant of 1 minute (Fig. 4)

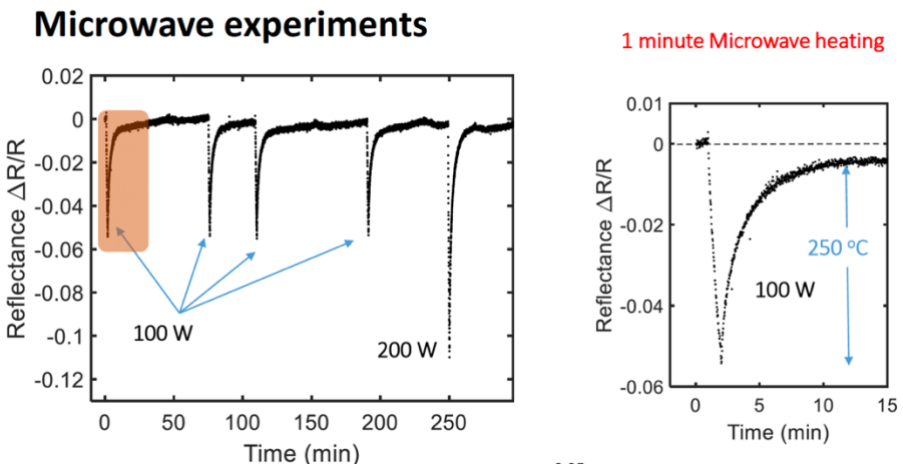

Figure 3. The rise in voltage ratio as measured in response to microwave heating of the glass slide coated with a thin layer of gold (inside newly designed microwave reactor). A temperature rise of 250°C within 1 minute was estimated.

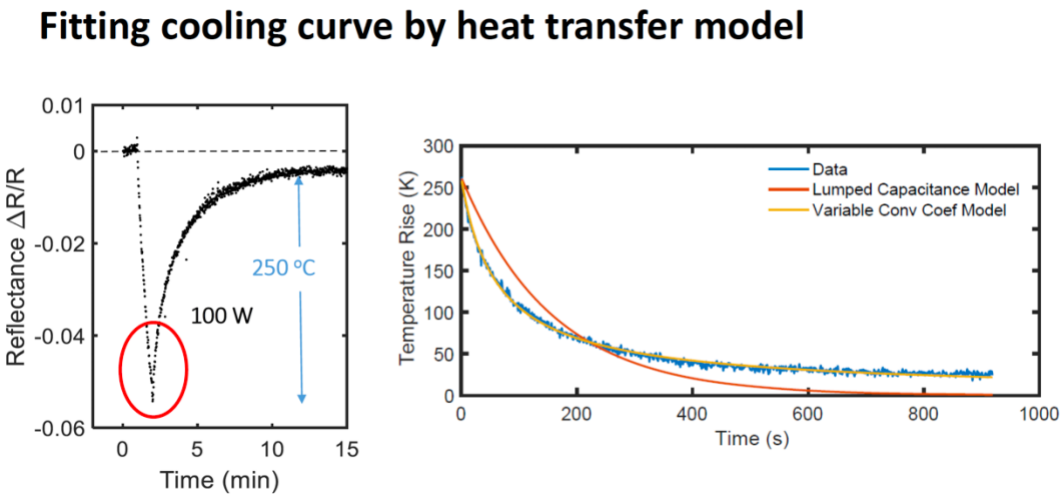

Figure 4. No sudden jump is seen on turning off the microwave reactor (left). Instead the exponential cooling curve can be fit to various heat transfer models (right) to determine the heat transfer mechanisms involved. These fits are ongoing.

While we could use the laser to measure temperature directly off of the Au surface, we could not do this when the beam was incident from the opposite side and first passed through the glass. The latter can become important during in-situ experiments. The thermal expansion of the glass likely causes variations in interference between the reflection from the Au and reflection from the glass itself that causes variability in the thermoreflectance signal. Our hypothesis is that this will be solved by using glass that has a wedge shaped cross section such that reflections from the front and backside diverge. This is the inspiration for the **Sample holder** design in Fig. 5:

Fig. 5a illustrates the sample holder by itself. Fig. 5b shows the same holder with both the cuvette and the wedged prism now in place. Fig. 5c depicts the cross-section orientation of the desired film growth. This holder is to both hold the Ti sol-gel precursor in place with a tight seal between the cuvette (shown in dark red) and the wedged prism (shown in light purple), and to allow laser light to reflect off the Au thin film as a way to measure temperature using thermoreflectance. Teflon was the material used to fabricate this part, which was done with local vendor company Conturo Prototyping.

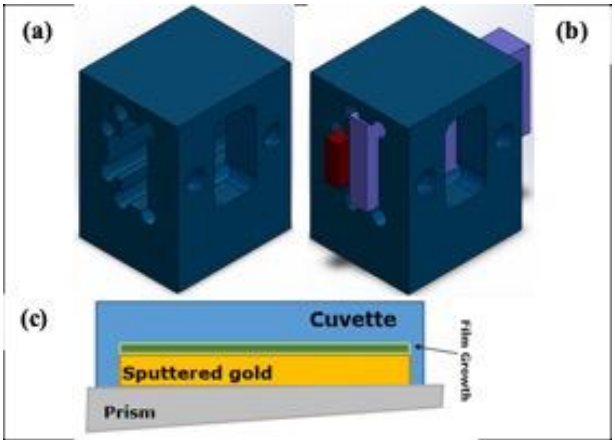

Figure 5. (a) *Sample holder in isometric view (b) sample holder with cuvette and wedged prism in isometric view (c) schematic of film growth oriented inside of a cuvette with the prism being used as sealant.*

Task Summary and next steps: The holder design work was done by a first year PhD student Malik Blackman. Professor Jonathan Malen (CMU, Mechanical Engineering) was an unpaid collaborator and co-adviser for the student. The PhD student did not pass the PhD qualifying exam and left the program in 2021. So we could not continue with in-situ temperature measurements during synthesis.

Objective 2 proposed to conduct in situ, operando synchrotron x-ray based investigations to determine the Effect of microwave radiation on altering the Arrhenius parameters like Gibbs free energy of activation and/or pre-exponential coefficient

The underlying mechanism of how electromagnetic (EM) fields, such as microwave radiation, affects the processing-structure-property relationships of a material has remained elusive due to the difficulty in differentiating between thermal (e.g., heating) and specific non-thermal field-driven structural effects. In earlier attempts, the two effects were differentiated by predicting actual temperature of reactants, which are inherently difficult to measure as the local temperature can be significantly different from macroscopic bulk temperature. These erroneous estimations have led to different conclusions about field-driven non-thermal effects. In our paper, we used *in-situ* Synchrotron X-ray diffraction experiments to understand the structural changes in the anatase phase of TiO_2, when exposed to microwave radiation (MWR). We show that MWR can nucleate defects in the lattice structure that can induce decrystallization (ordered-disordered phase transformation) and **anisotropic lattice expansion**, which is not related to the thermal effect of MWR. Molecular dynamics simulations demonstrate that introducing an oxygen vacancy in the anatase structure results in the formation of a vacancy-interstitial pair. This observation could

explain the anisotropic expansion of anatase, if MWR could indeed induce sufficient amount of defects in the structure. By utilizing *in-situ* characterization techniques and simulations, we provide direct evidence for non-thermal coupling between EM fields and matter through defect-mediated anisotropic expansion-contraction.

We will now describe some of the major results in detail here. Our results were published in **[Paper 1]**

***1. In-situ* X-ray diffraction:** We performed two types of *in-situ* diffraction experiments using the high energy synchrotron X-rays at beamline 6-ID of the Advanced Photon Source (APS) at Argonne National Laboratory (ANL) (see schematic in Fig. 6): (a) microwave radiation (MWR)-heating of anatase TiO_2 powders (no synthesis involved) and (b) synthesis of anatase powders from the growth solution under MWR-assisted heating. During MWR-assisted heating of anatase powders, we track the change in lattice parameters while the powder is being heated. For MWR-assisted synthesis experiments, the diffraction peaks of anatase appear only after a sufficient amount of the powder has nucleated in the solution, i.e. when the solution temperature reaches 150°C (see paper for details). Since the diffraction spectrum also includes scattering from the glass vial and the solution, a large amorphous hump is also detected as background. A high order polynomial fitting is used to filter out the Gaussian diffraction peaks of the crystalline materials.

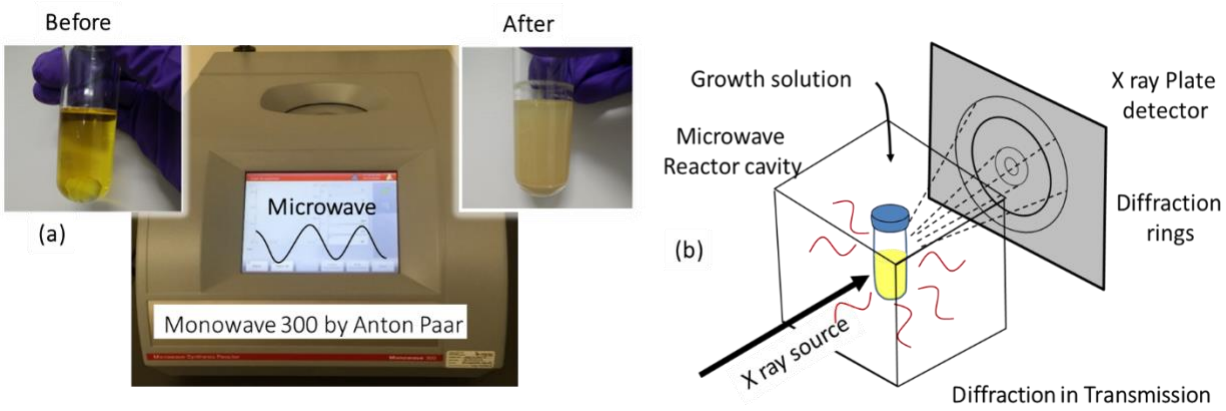

Figure 6. Schematic of the experimental setup for MWR assisted synthesis experiments. (a) Anton Paar Monowave 300 microwave reactor, with tetraethylene glycol (TEG)/sol-gel precursor mixture before and after synthesis. (b) *In-situ* diffraction set up at beamline 6 ID-D, APS. The precursor solution is placed in a microwave reactor with ports cut out for X-ray inlet/outlet. The high energy X-rays enter from the front side of the microwave-reactor and get diffracted in transmission mode on the plate detector.

We find that the lattice parameters ('*a*' and '*c*') of the as-received reference powder of anatase expands when heated up to 300°C in a conventional furnace. The lattice expands linearly with the thermal expansion coefficient of 2.5×10^{-5} and 5.0×10^{-5} /°C in '*a*' and '*c*' directions respectively. These values match closely with the previously estimated lattice expansion coefficient of anatase. When the same as-received anatase reference powders were heated with MWR up to 250°C, we observe a non-linear expansion-contraction in the lattice parameters as shown in Fig. 7a. The horizontal axis used here is *time* instead of *temperature* because the MWR heating profile is not

linear. We find that initially the lattice shrinks until a temperature of 180°C is reached (time 100 min) followed by expansion to the point of maximum temperature of 250°C. This non-monotonic expansion-contraction could be the combined result of thermal expansion and field-driven contraction of unit-cells. Overall, there is a volume contraction of the anatase unit cell, Fig. 7b, which does not follow the solution temperature as recorded by the IR sensor during the experiment. Interestingly, a similar effect of anisotropic expansion in '*a*' and '*c*' has been seen in sintering of 3 mol% yttria-stabilized zirconia (3YSZ) under a direct electric (DC) field (in flash sintering), which was suggested to be the result of non-thermal defects in the structure under externally applied fields. Additionally, we observe an instantaneous reduction in the intensity of the (101) peak within 2 minutes of MWR exposure, while the full-width-half-maxima (FWHM) remains relatively unchanged, as shown in Fig. 7c. Comparing the entire diffraction pattern before and during MWR-heating reveals a systematic reduction of peak intensity, Fig. 7d, which is an indication of decrystallization (ordered-disordered phase transformation). It is known that rapid heating under MWR results in random displacement of atoms, thus creating lattice strain. This decrystallization, or formation of the amorphous phase, can also be thought of as the generation of a highly distorted lattice structure due to the formation of a high concentration of defects (vacancies and interstitials) under the field.

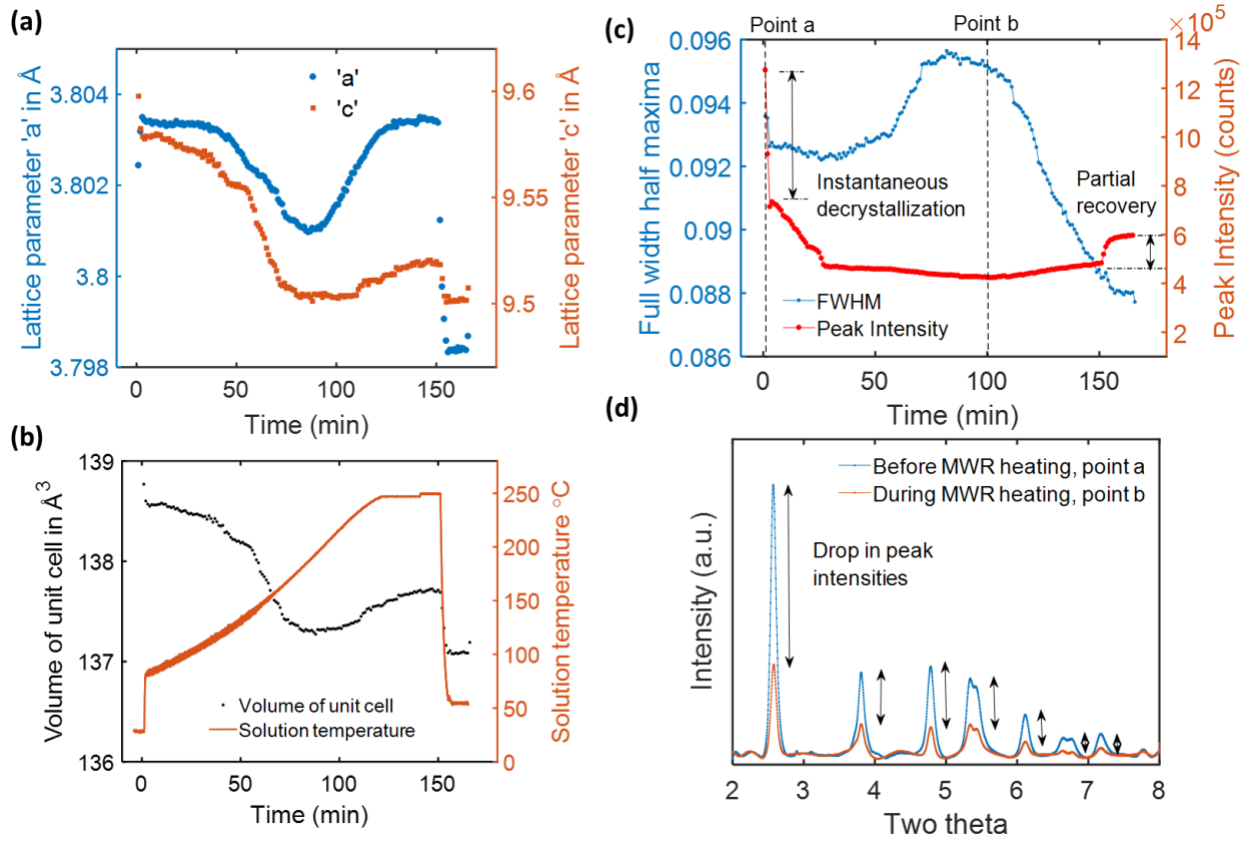

Figure 7. A MWR-heating experiment of as-received reference anatase powder that was dispersed in a solution of tetraethylene glycol (TEG). (a) The change in lattice parameters '*a*' and '*c*' as a function of time. While the solution temperature continues to rise monotonically, both the lattice

parameters shrink until a temperature of 180°C is reached (time = 100 min), at which point the lattice starts expanding. We consider that there are two phenomena operational: thermal expansion because of rise in temperature and lattice contraction under EM field. At any point during the experiment, the resultant lattice parameter depends on which of these two factors is dominant. Once the MWR is switched off at 150 minutes, both the lattice parameters shrink immediately, but they do not go back to their starting lattice parameters at room temperature, which is an indication of non-equilibrium defects that are kinetically constrained to annihilate and left behind in the structure. (b) The calculated unit cell volume and temperature profile plotted versus the duration of the synthesis experiment. The total duration of the MWR heating is 150 min, starting at a time of 2 minutes. (c) shows the sudden drop in the peak intensity of (101) within the first 2 scans (first 2 minutes of MWR exposure), while the FWHM remains unchanged. Subplot (d) compares the diffraction patterns at the beginning of the experiment (refer to point a of subplot c) and during MWR-heating at a time of 100 minutes (which corresponds to point b of subplot c). A systematic decrease in the intensities of all the peaks suggests decrystallization.

Based on the experimental results shown above, we hypothesize that MWR-assisted synthesis and MWR-heating lead to defect generation, such as the nucleation of oxygen vacancy-interstitial pairs, which are examples of field driven non-thermal effects. To test this hypothesis, molecular dynamics (MD) simulation was used to probe the mobility of atoms around an oxygen vacancy in the anatase structure of TiO_2, as discussed below.

2. Molecular dynamics (MD) simulation: The second-moment tight-binding charge equilibration (SMTB-Q) potential model is used to describe the iono-covalent bonding in anatase TiO_2. This potential allows for the redistribution of the ionic charges based on the local environment at every time step, which allows changes in the local charge distribution due to defects to be effectively accounted for. On introducing an oxygen vacancy at lattice site 1 (Fig. 8a), the neighboring oxygen quickly moves from its position at lattice site 2 and forms a stable interstitial in the middle of lattice site 1 and lattice site 2 (Fig. 8b and 8c). The simulation thus suggests that if an externally applied field (MWR in our case) can indeed nucleate vacancies, then the nearby oxygen atom will form an addition interstitial-vacancy pair to minimize the potential energy. This understanding is aligned with the idea of oxygen vacancies found in non-stoichiometric TiO_2 and at the same time agrees with the peaks corresponding to oxygen interstitials seen under other characterization like x-ray photoelectron spectroscopy (XPS) – see paper for details. Because the volume was kept constant during the simulation, there is no change in the lattice parameters. However, if MWR could nucleate enough defects, distortion in the lattice structure of anatase is possible, as observed during *in-situ* diffraction experiments.

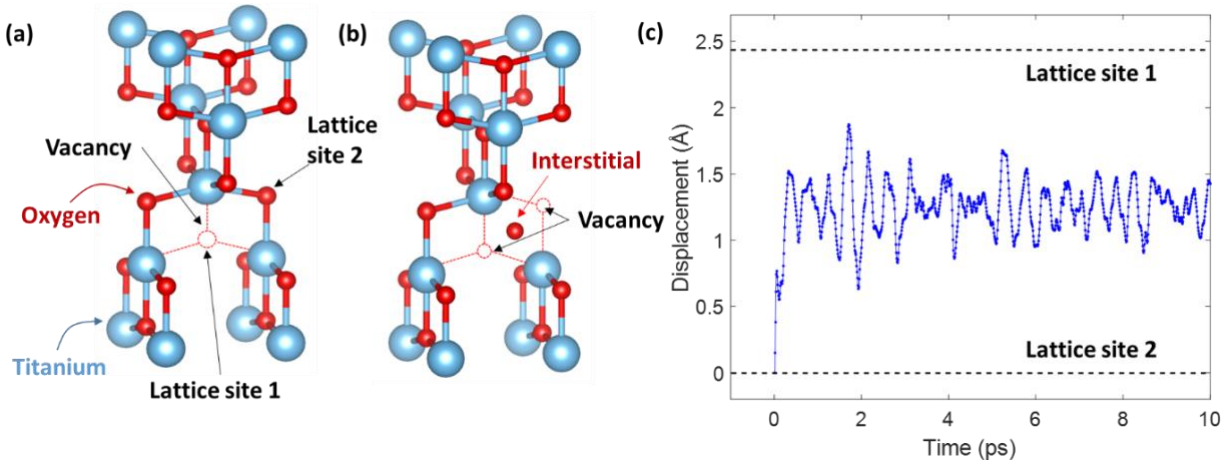

Figure 8. (a) An anatase unit cell with an oxygen vacancy introduced at lattice site 1 at the beginning of the simulation. (b) During the simulation, the neighboring oxygen atom at lattice site 2 moves to a position approximately halfway between lattice site 1 and lattice site 2 and remains there as an interstitial, leaving behind another vacancy. (c) Displacement of the oxygen atom from its original position (lattice site 2), as obtained from an MD simulation to a final position between lattice site 1 and lattice site 2. This result thus suggests that if an externally applied field (MWR in our case) can nucleate a vacancy, then the nearby oxygen-atom will form an addition interstitial-vacancy pair to stabilize the structure. The structures shown in (a) and (b) were generated using VESTA®, where the red spheres represent O atoms and the blue spheres represent Ti atoms. A video of the transition for the full 1764 atom simulation box is provided in the paper.

3. Estimating the activation energy and the pre-exponential factor – This task was suspended for 2 years due to CCOVID-19 access restriction at Brookhaven National Lab. A new PhD student Morgan Chen (on an internal CMU fellowship in 2020-21) was briefly added to the project. Morgan worked with undergraduate student Colby Sisco to upgrade the microwave reactor hardware and software. Even though the project has ended Morgan will perform in-situ experiments to measure kinetic parameters such as Gibbs free energy of activation during a visit to the beamline in Dec 2022, supported by PI Jayan's discretionary funding. Two manuscripts will be written based on this work, which will be send to the ARO repository, when published. Some details of these experiments are briefly summarized under Objective 3, Pump-probe time-resolved x-ray studies.

Objective 3 proposes to identify *far-from-equilibrium* effects and relate them to the microwave radiation field parameters

High resolution transmission electron microscopy (TEM) imaging confirm results from Objective 2, that MWR-induced decrystallization leads to a mixed amorphous-crystalline microstructure, which could be a signature of the non-thermal field-driven effects. The results from XPS and Raman spectroscopy) further suggest the formation of oxygen vacancy-interstitial defects in the lattice, which agree with reports from other field-assisted processing techniques such as flash sintering. We will now describe some of the major results in detail here. Our results were published in **[Paper 1]**

1. Microstructure Characterization: High resolution TEM images and insets of the local fast Fourier transformation (FFT) of as-received, MWR-heated, and MWR-synthesized anatase powders are shown in Fig. 9a-c. The as-received powder contains crystalline nanodomains, which is consistent with the clearly distinguished diffraction spots in the local FFT. The MWR-heated powders contain amorphous-crystalline mixed regions and the FFT did not have clear spots. MWR-synthesized powders are similar to the as-received anatase sample, as it shows mixture of amorphous and crystalline nanodomains with distinguishable spots in the local FFT.

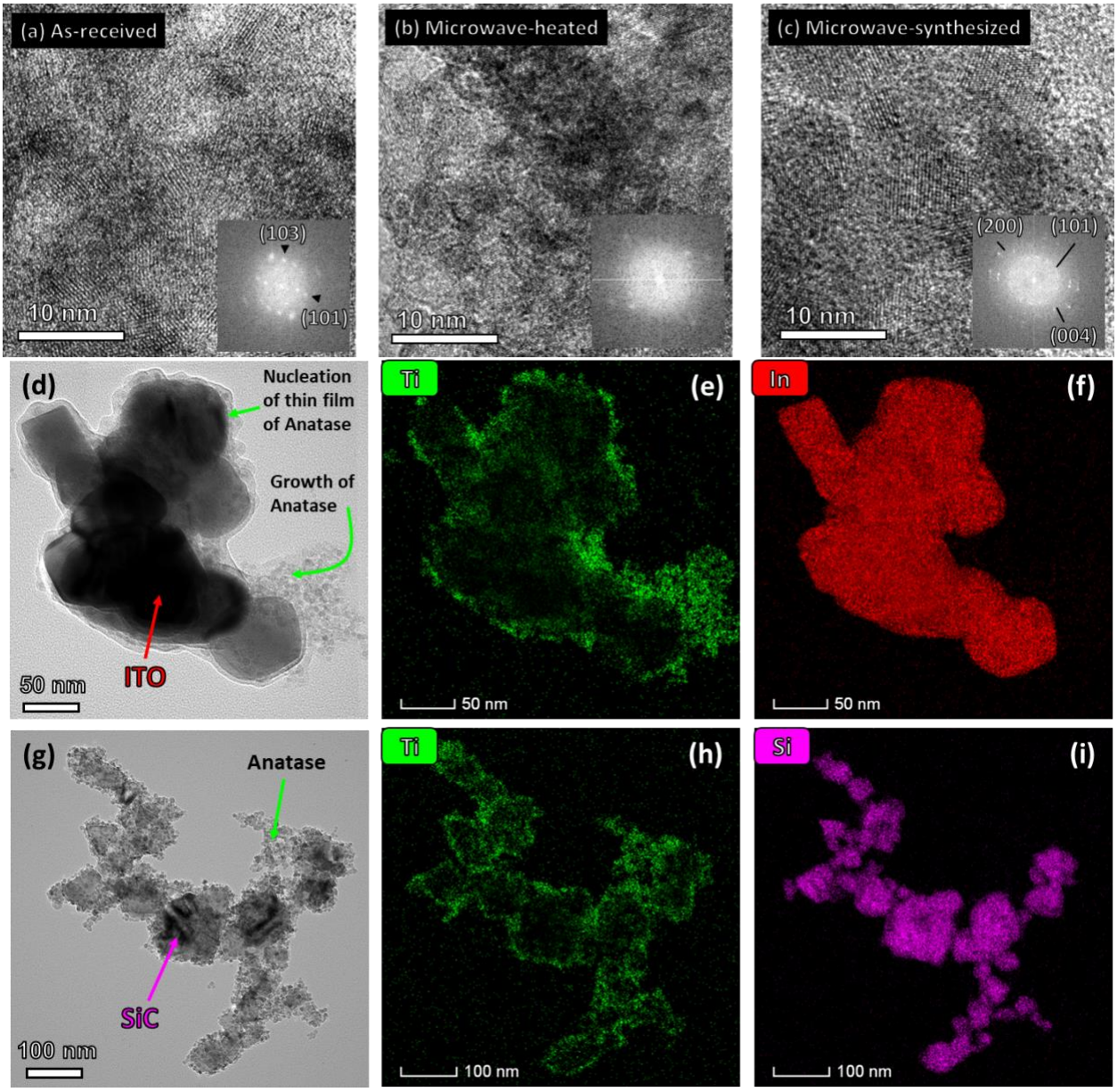

Figure 9. High-resolution transmission electron micrographs (HRTEM) of the (a) as-received anatase powder, (b) anatase powder after being heated with MWR, and (c) MWR-synthesized anatase powders from sol-gel growth solution. The insets correspond to the local fast Fourier

transformation (FFT), which have been indexed with diffraction planes corresponding to anatase. (d) High magnification image of susceptor (ITO) particles shows a thin film of TiO_2 and agglomerated particles, as observed by the energy dispersive spectroscopy (EDS) images of the same particle for Ti (e) and In (f). (g) shows nucleation of nanaoparticles of TiO_2 on SiC susceptors and the EDS image for Ti (h) and Si (i). Although EDS only gives the elemental composition, we used the results of *in-situ* diffraction experiments and TEM FFT studies to assume that the thin film/agglomerate is the anatase phase of TiO_2.

The MWR-assisted synthesized powders are still more amorphous than reference (as-received) anatase powders. It should be kept in mind that TEM imaging is location specific and does not represent the entire powder, whereas XRD represents diffraction patterns of the entire volume when done in transmission mode (as was the case for our experiments). The average particle sizes are in the range of 4-8 nm for all three conditions. These results support the hypothesis of decrystallization, which is also confirmed from *in-situ* and laboratory diffraction results. In the experiments involving sensitizer or susceptor particles that can specifically attract the microwave field, Fig. 9d and 9g, we see nucleation of an anatase thin film on the susceptor surface followed by agglomeration of anatase nanoparticles. Subplots (e) and (f) are the elemental maps of Ti and In for indium tin oxide (ITO) aided anatase synthesis. Subplot (h) and (i) are the elemental maps of Ti and Si for SiC aided anatase synthesis. The elemental maps help us to outline the sensitizer or susceptor materials from the synthesized anatase. We conclude from these images that sensitizer or susceptor act as nucleation sites in the early stages of microwave heating, as had been suggested by *in-situ* diffraction studies of Fig. 7.

2. Multiscale computational modeling

- **Finite element methods in COMSOL to simulate the standing-wave in the microwave cavity *(CONTINUUM SCALE)***

An electrically conducting sensitizer/susceptor like ITO or Au acts like an antenna and preferentially absorbs microwaves, helping to promote nucleation and growth. Using COMSOL Multiphysics, we simulated the field absorption in various layers (both conducting and semi-conducting) across a range of EM field input conditions, allowing us to systematically study how experimental conditions influence the field-assisted synthesis.

Our COMSOL simulations indicate non-uniform EM field absorption in the ITO layer, as expected. When microwaves at a frequency of 2.45 GHz and 800 W power is exposed to a 0.5 mm thick rectangular ITO layer, we observed significantly enhanced field absorption along the longer edge (Fig. 10a). This aligns well with previous literature regarding the behavior of EM fields at edges, and corresponds to regions with thicker thin film growth. Interestingly, in square ITO layers, we find that the maximum field intensity is higher in the surrounding solution ($9.0x10^4$ V/m) than in the ITO layer ($3.7x10^4$ V/m), suggesting that absorption by the ITO layer serves to enhance the electric field intensity in the nearby solution (Fig. 10b,c). In addition to ITO, we also modeled EM field absorption on non-conducting ZrO_2 layers in precursor solutions identical to those used in the studies with ITO. The ZrO_2 layer results in a lower maximum electric field intensity ($7.0x10^3$ V/m) and promotes a different field distribution than what is found in ITO (Fig. 10d).

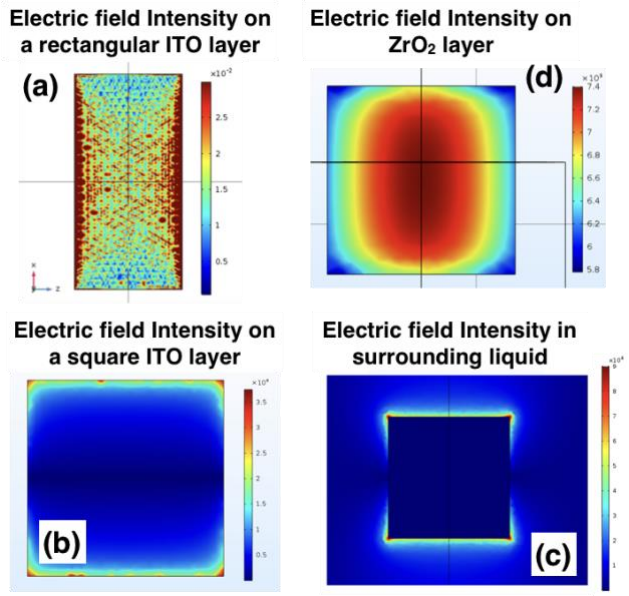

Figure 10: *COMSOL Multiphysics simulations of electric fields induced by microwave radiation on various materials (a, b) conducting ITO, (c) dielectric solution, (d) non-conducting ZrO_2 and on varying substrate shapes (a) rectangle and (b) square. Color scale shows electric field intensity with red being highest intensity.*

These results clearly demonstrate that by tailoring both shape and material properties (e.g., dielectric constant) of the substrate layer, electric field intensities and distributions (accordingly heat buildup and local temperatures) on the sensitizer surfaces can be modified to influence nucleation and growth. This matches with the results from laser thermoreflectance measurements in Objective 1.

- **Pair distribution function analysis of defects in microwave radiation synthesized TiO_2 and ZrO_2 – enabled by molecular dynamics simulations (ATOMISTIC SCALE)**

The atomic structure of a high-quality single crystal can be obtained from X-ray diffraction (XRD), which measures the Bragg peaks that result from the atomic periodicity. XRD is not sufficient for specifying the atomic structure of nanocrystalline and/or highly defected samples. Pair distribution function (PDF) analysis uses data from total scattering experiments (i.e. both Bragg scattering and diffuse scattering is collected) , the latter of which results from disorder, and allows for structural characterization without assuming periodicity. The PDF is thus a powerful tool for quantitatively characterizing short-range and long-range atomic structure. A major challenge in PDF studies is to match the experimental data with a model structure; an iterative and time consuming, slow process called refinement. PDF refinement involves the selection of the starting atomic structure when the material and phase are already known and detailed structural information is required. Atomistic simulations provide a solution to this challenge and can help speed up the quantification of structure from PDF data. While density functional theory (DFT) can perform first principles-based energy calculations, it is limited to small systems with minimal complexity by its large computational cost. Empirical interatomic potentials, on the other hand, can efficiently provide the

total energy of a large, complex system as an explicit function of its atomic coordinates. A well-parameterized potential can maintain high accuracy when compared to a DFT calculation.

Measured PDFs of anatase titanium dioxide (TiO_2) and tetragonal zirconium dioxide (ZrO_2) grown in the presence of microwave radiation (MWR) are used to demonstrate this method. External fields can induce defects that alter the diffusion of space charges across grain boundaries and ultimately lead to efficient processing. **Our goal was to identify the types and concentrations of point defects that are present in MWR-grown anatase TiO_2 and tetragonal ZrO_2.** While we focus on structures with local disorder, this workflow can also benefit PDF analysis of nanoparticles and perovskites, which are challenging to characterize using conventional methods. Details can be found in our manuscript **[Paper 3]** currently in peer review. Professor Alan McGaughey was an unpaid collaborator on the MD simulation work.

Method 1 - Atomistic calculations and structure model generation: We used an empirical potential to relax the defected structures and generate structure model for PDF refinement. The potential is called second moment tight binding charge equilibrium potential, or SMTB-Q, which allows for the redistribution of charges based on the local environment. We built structures with different types and concentrations of randomly placed point defects and relaxed them at zero temperature by energy minimization. To investigate the sensitivity of the refined PDF to the defect locations, ten structures were created for each configuration. We consider common point defects for both the cation (Ti and Zr) and the anion (O): vacancies, interstitials, Frenkel pairs (a cation vacancy and interstitial pair), and anti-Frenkel pairs (an anion vacancy and interstitial pair), and combinations of these defect types.

Method 2 - Pair distribution function (PDF) analysis: The PDF refinement is performed using the DiffPy-cmi software package, that is open source. The structure models are fit against the measured PDFs by refining global and phase-specific scaling factors, lattice parameters, isotropic atomic displacement parameters (ADPs, denoted by U_{iso}), a low-r peak sharpening coefficient for correlated motion of nearby atoms, and a PDF peak envelope function, which dampens the signal as a function of separation to account for grain/particle size. The quality of the fit is quantified by a goodness-of-fit value R_w, which is calculated as,

$$R_{\mathrm{w}} = \sqrt{\frac{\sum_n (G_{\mathrm{obs},n} - G_{\mathrm{calc},n})^2}{\sum_n G_{\mathrm{obs},n}{}^2}}$$

Results on TiO_2 - The five contour plots containing the lowest R_w values are shown in Figs.11a-e. The lowest fitting error R_w (0.264) corresponds to the structure with 3.40% Ti vacancies, 1.70% Ti interstitials, and 0.28% O interstitials [indicated by the red star marker in Fig.11a]. Six other defected structures give a similar R_w (within 3% of 0.264) after the PDF refinement [indicated by red square markers in Figs.11a-e]. All of these structures have the Ti vacancy as the dominant defect type, followed by the Ti interstitial.

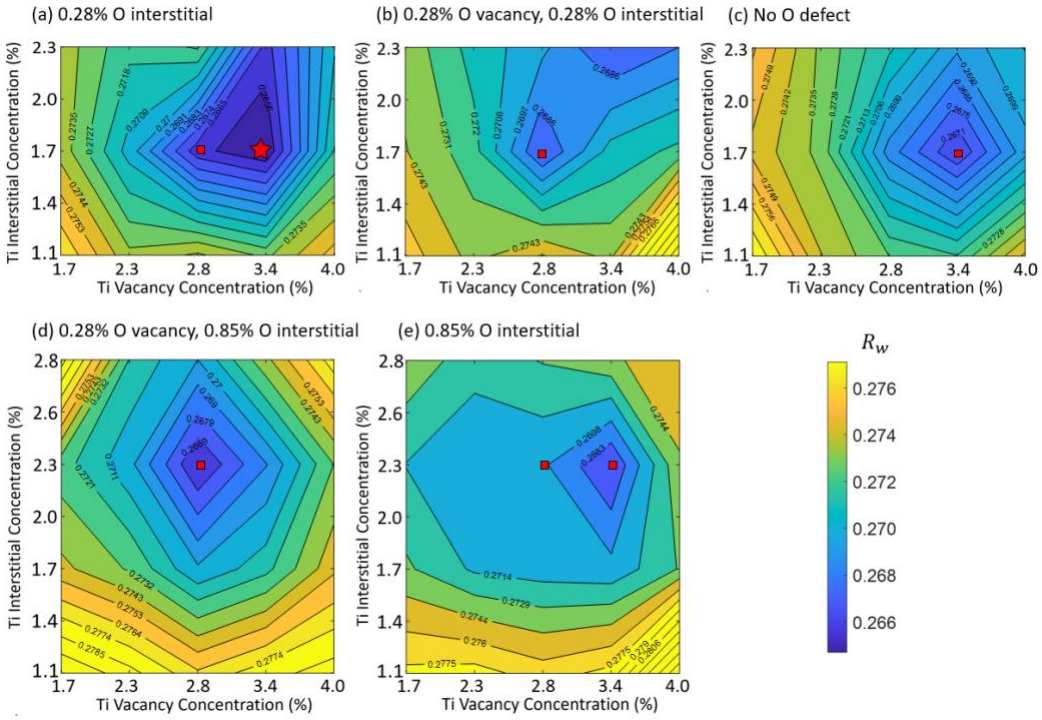

Figure 11. PDF refinement for anatase TiO_2 separated into short, medium, and long-range order. The green curves are the differences between the refined and experimental PDFs. (a)-(c) are the refined PDFs using the perfect structure and (d)-(f) are the refined PDFs using the defected structure with the lowest R_w.

Results on ZrO_2 - The resulting two-dimensional R_w contour is shown in Fig. 12. The lowest R_w (0.214) results for the structure with 4.8% O vacancies and no O interstitials (indicated by the red star marker in Fig. 12). Four other defected tetragonal ZrO_2 structures give a similar R_w (within 1% of 0.214) after the PDF refinement. All of these structures have the O vacancy as the dominant defect type, followed by the O interstitial.

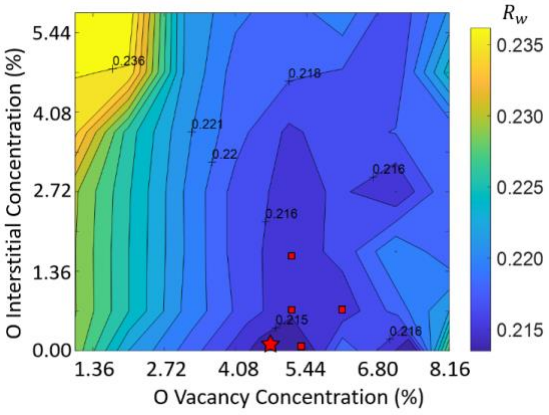

Figure 12. Variation of R_w with O defect concentration for tetragonal ZrO_2. The red markers indicate the five lowest R_w values. The lowest R_w, the red star, results from the PDF refinement of a structure model with 4.8% O vacancies.

- **Data-driven Pair Distribution Function Analysis for Oxide Defect Concentration Identification – for autonomous experimentation platforms for materials discovery**

Advances in synchrotron X-ray scattering experiments have greatly increased the acquisition rates of pair distribution function (PDF) data. The analysis and interpretation of the data, however, are lagging behind the experimental advances because PDF analysis is met by the challenge of finding the correct structure model to fit against the data, which is a time-consuming process. An experimentally measured PDF can be analyzed by adjusting the parameters of an assumed structural model, such as the lattice constants, atomic positions, and grain/particle size. A refined PDF is obtained by minimizing the difference between the PDFs of a structural model and the experimental PDFs. A real-space Rietveld method was implemented by us to perform this analysis in PDFgui, DiffPy-cmi and TOPAS.A major challenge in PDF modeling is the selection of the starting atomic structure. Significant information about the sample (e.g., the crystal phase) is required to achieve satisfactory results. Typically, PDF modeling thus involves manual trial-and-error refinement of multiple structural models. There have been attempts to automate and accelerate this process, where a large number of structures are either pulled from a materials database or generated automatically. These approaches, however, may not be sufficient for in-situ PDF measurements of which captures the material composition and structural change over time, where large number of PDFs would need to be analyzed one at a time.

We tried to apply data driven methods and machine learning instead of traditional PDF analysis to characterize local material structures. As reported in the previous sections, MWR may lead to defect generation during MWR-assisted synthesis of anatase TiO_2. It is important to identify the types and concentrations of point defect present in the MWR-grown TiO_2 as it may help us understand the mechanisms of field effects. Here, **we use machine learning based feature engineering algorithms to extract features and reduce dimensions from and of the dataset containing simulated PDFs of defected anatase TiO_2.** A neural network (NN) is then trained using the reduced data as input to predict the defect concentration. The trained model is then used to predict the defect concentration of experimentally measured PDFs of anatase TiO_2. We compare the performance of different dimensionality reduction techniques by analyzing the extracted features from the simulated PDF dataset. Details can be found in our manuscript **[Paper 4]** currently in peer review. Professor Alan McGaughey was an unpaid collaborator on the simulation work.

Method 1: Principal component analysis (PCA) and non-negative matrix factorization (NMF): Both PCA and NMF can be described in the framework of matrix factorization. The dataset can be regarded as a matrix V of dimensions $n \times m$, each column of which represents the m points on a PDF curve. The r columns of W which is in dimension $n \times r$ matrix are the basis of V. The r rows of matrix H which is in dimension $r \times m$ represent the weight associated with the bases. $V \approx WH$

The difference between PCA and NMF lies in the constrained applied to the matrix factors W and H. In PCA, the columns of W (the principal components) are constrained to be orthonormal and the rows of H to be orthogonal to each other. In NMF, the elements in W and H are constrained to be non-negative.

Method 2: Autoencoder: Autoencoder is an unsupervised learning technique in which we leverage neural networks for the task of representation learning. A NN architecture is constructed

such that we impose a bottleneck in the network which forces a compressed knowledge representation of the original input. In this case, the inputs are the simulated PDFs of defected anatase. The extracted features are embedded in the hidden layer of the autoencoder. It has been reported that a single hidden layer autoencoder is very similar to NMF theoretically. A softplus activation function is applied at the hidden layer to ensure the positivity of the latent space *H*. This autoencoder is similar to the NMF algorithm in that the weights **W** in the decoder layer can be interpreted as the basis PDFs and the latent space *H* is the activation associated with the basis PDFs. The product of **W** and *H* approximate the original PDFs. This model can also be easily extended to a multilayer autoencoder by adding more layers to the NN architecture to achieve a nonlinear representation of the feature space.

Results – We find that non-linear models provide predictive capability while linear models without physics awareness are merely capable of interpreting/feature extracting tasks. Details are summarized below

- Feature extraction

Fig.13 shows the first five columns of the **W** matrix from NMF (green dashed curves) and the first five columns of the decoder weights from the single-layer autoencoder (red curves). The blue curve in Fig. 13a is the PDF of perfect anatase, and the blue curves in b-e are the PDF contribution of the four types of defects, calculated by subtracting the PDFs of perfect anatase from the defected anatase with certain point defect. It can be seen that the features extracted by autoencoder match the PDF signal of the perfect phase and the defects better. This result indicates that autoencoder with a single hidden layer can extract features that are more physically interpretable. This may be caused by the fact that in NMF, the elements of the data matrix and the decomposed matrices **W** and **H** need to be non-negative. In reality, however, the basis PDFs, i.e., the columns of the **W** matrix have no reason to be non-negative. While in the autoencoder, there is no such constraint applied on the basis PDFs, i.e., the decoder weights.

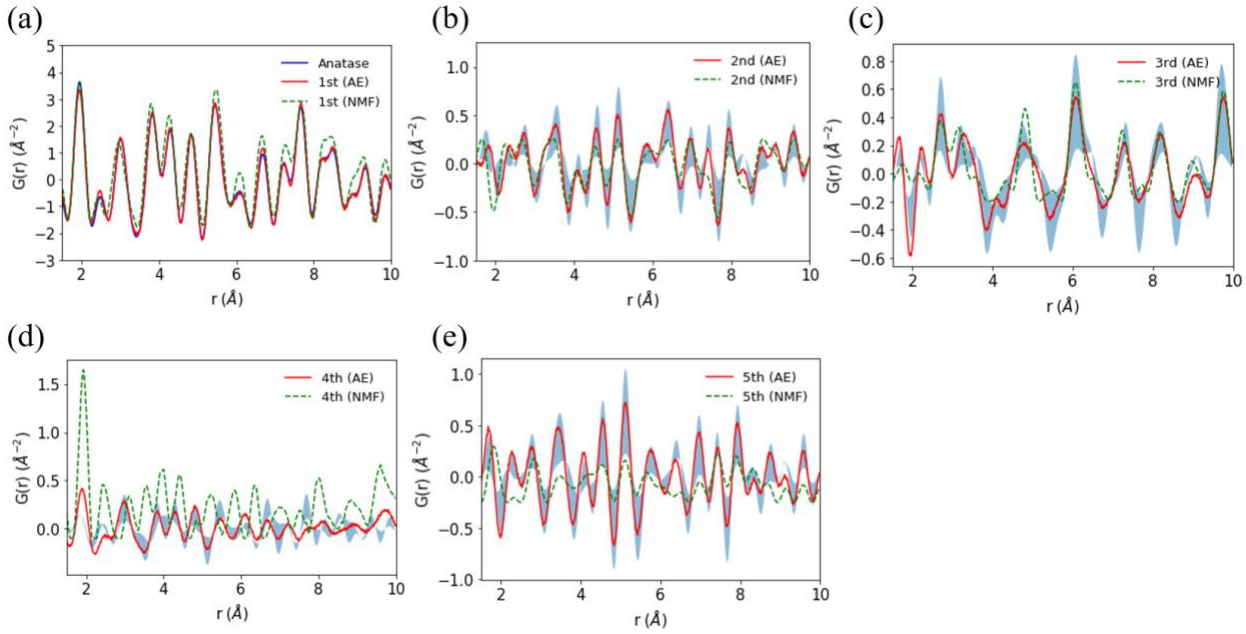

Figure 13. The first five columns of the **W** matrix from NMF (green dashed curves) and the first five columns of the decoder weights from the single-layer autoencoder (red curves), i.e., the PDF signal of (a) the perfect anatase phase, (b) Ti vacancy, (c) Ti interstitial, (d) O vacancy, and (e) O interstitial.

- Prediction on experimental PDFs

The reduced PDF data (the **H** matrix from NMF, the latent dimension from autoencoder, etc.) are then used as input to a NN that maps to the defect concentration of the four defect types. Fig. 14 shows the prediction results of the defect concentration of a microwave grown anatase sample that has been previously studied in our group using conventional PDF analysis. A total of five feature extraction methods are compared, namely PCA, NMF, single-layer autoencoder, multilayer autoencoder, and the convolution layer of convolutional neural network (CNN). The results generated from using no feature extraction are shown on the far left of the figures as reference. The red strips indicate the defect concentrations determined by conventional PDF analysis. **The predictions by the single-layer autoencoder are the closest to the previous study, suggesting that using a physically interpretable feature as the input to a model can increase the predicting ability of a model.**

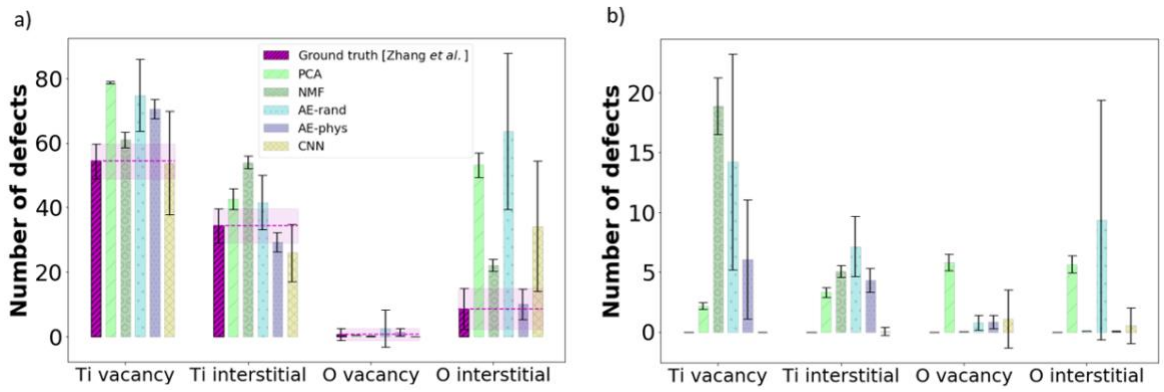

Figure 14. Predicted number of defects in an initially perfect 1944-atom cell for experimental TiO_2 PDFs using PCA, NMF, AE-rand, AE-phys, and 1D-CNN along with the ground truth for (a) a defected anatase TiO_2 sample from our previous work and (b) a perfect anatase TiO_2 sample. The bar graphs show the mean and the standard deviation for each type of model trained 50 times with different random seeds.

3. Microwave Pump-X-ray probe time-resolved studies

The nature of the interactions between microwave radiation and matter that give rise to technologically appealing phenomena, such as reduced processing temperatures/times or enhanced product properties, remains unclear. Clarifying the influence of microwave radiation in materials synthesis has been hindered by a lack of instrumentation to study structural transitions in situ and structural alterations on the atomic scale. Therefore, this task (which was delayed during COVID restrictions at the beamline) is to help elucidate the role of the microwave field in materials synthesis by probing the kinetics and energy landscape of microwave-induced reactions via in-situ, atomic characterization techniques. A bespoke 2.45 GHz microwave reactor and modular flow-through system was developed to enable high throughput, in-situ microwave studies. Furthermore, this system is deployed at a synchrotron beamline (BNL, NSLS-II, 28-ID-2 XPD) to utilize high-energy (~68 KeV) X-rays that can resolve atomic dimensions, as shown in Fig.15.

To leverage the synchrotron X-rays for investigating specific nonthermal microwave effects that may reside in the atomistic domain, this experimental platform is coupled with the atomic pair distribution function analysis (PDF) technique that is well suited for quantitatively characterizing local structural fluctuations in the atomic environment – from amorphous precursors to partially crystalline intermediary phases leading to the final crystalline powder product. Using total scattering with PDF analysis contrasts with conventional X-ray diffraction (XRD) measurements, which are applicable for characterizing well-ordered phases and long-range crystallinity but are ill-equipped for studying mixed amorphous-crystalline samples and features on the nanoscale.

In sum, a custom microwave system enabling in-situ PDF analysis will be installed at the NSLS-II x-ray synchrotron beamline 28-ID-2 to monitor and compare the synthesis of Tin oxide nanoparticles via microwave-assisted and hydrothermal methods at varying temperatures. An Arrhenius plot will be generated from the experiments to isolate the activation energies of the reactions. The hypothesis is that microwave-assisted synthesis of Tin oxide nanoparticles manifest lower activation energies than that of conventional hydrothermal synthesis, suggesting that

microwave irradiation promotes chemical reactions by lowering the energy barrier to product conversions.

Our novel experimental platform (combining X-ray probes with microwave sources) can in future be expanded to other synthetic systems that would benefit from high analytical temporal/spatial resolution. A better understanding of the unique role of the microwave field in materials synthesis is a requisite step towards furthering its widespread application in accessing novel materials and disruptive processing advantages.

A manuscript is in preparation and also submitted to the ECI conference on Electric Field Enhanced Processing of Advanced Materials III in Portugal in March 2023.

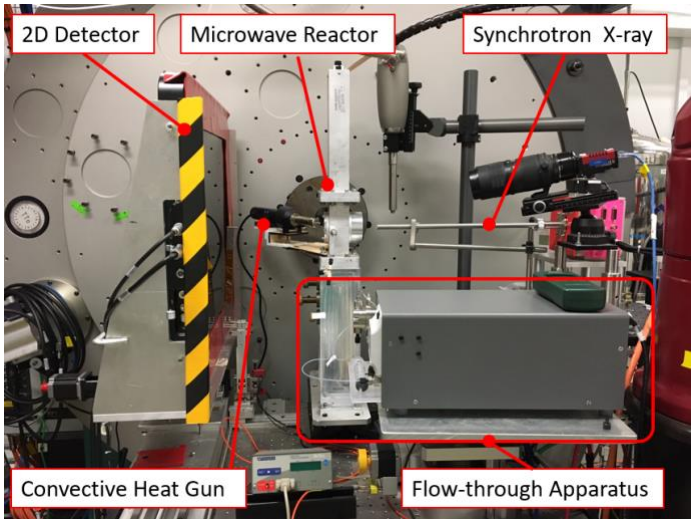

Figure 15. In-situ microwave experimental setup at the synchrotron beamline incorporating new flow-through synthesis capabilities

7. Conclusion

This grant allowed us to conduct high risk experiments that for the first time showed that microwave fields non-thermal affect the lattice of a crystal. Over 3 years, we quantified this effect at multiple scales. Using synchrotron x-rays we demonstrated that a unit cell exposed to microwaves heats up but shows anisotropic changes in its lattice parameters. One the contrary, conventionally applied heat shows a linear relationship between lattice parameters and temperature. We performed seminar laser thermoreflectance measurements to quantify the temperature spikes (up to 250 ^{o}C) seen on a macroscale strip of gold under microwaves. However, instantaneous values of temperature could have been much higher; but our instrument lacked the required temporal resolution. We used molecular dynamics simulations along with machine learning models to demonstrate that such field driven structural changes (that eventually disorder or even decrystallize the material) are a result of various types of defects being generated. Ongoing and future work will use this knowledge and the computational workflows we developed for autonomous materials synthesis and processing; an emerging paradigm for materials science. Through this grant, PI Jayan was able to establish relationships with national labs to take these efforts forward in the future *to discover materials unavailable to conventional routes.*